On complexified tetrahedron for double twist knot

Jun Murakami
Waseda University

1 Introduction

We explain a way to prove the volume conjecture for hyperbolic double twist knots by using the complex tetrahedron associated with the geometric $\mathrm{SL}(2,\mathbb{C})$ representation of the fundamental group of the complements. The volume conjecture for knots and links is the following, which is based on Kashaev's conjecture proposed in [4].

Conjecture 1 (Volume conjecture [6])**.** For a knot or link K,

$$2\,\pi \lim_{N\to\infty} \frac{|J_{N-1}(K)|}{N} = v_3\,||S^3 \setminus K||$$

where v_3 is the volume of the regular ideal tetrahedron and $||S^3 \setminus K||$ is Gromov's simplicial volume of the complement, which is the sum of Gromov's simplicial volumes of hyperbolic pieces of the JSJ decomposition of $S^3 \setminus K$.

This conjecture is generalized as follows.

Conjecture 2 (Complexified volume conjecture [7])**.** For a hyperbolic knot or link K,

$$2\,\pi \lim_{N\to\infty} \frac{J_{N-1}(K)}{N} = \mathrm{Vol}(S^3 \setminus K) + \sqrt{-1}\,\mathrm{CS}(S^3 \setminus K)$$

where $\mathrm{CS}(S^3 \setminus K)$ is the Chern-Simons invariant and $\mathrm{Vol}(S^3 \setminus K)$ is the hyperbolic volume of the complement.

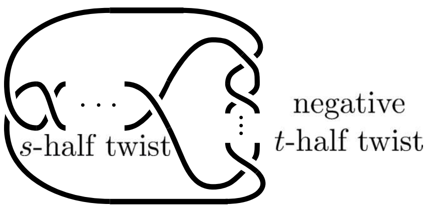

Figure 1: (k,t) double twist knot or link K. K is a link If s and t are both odd, then K is a link, and if otherwise K is a knot.

Here we investigate (s,t) double twist knot given in Figure 1. Conjecture 2 is solved for some knots and links, but not so much. For the figure eight knot, it is easy to prove by undergraduate calculus. Proofs for other prime knots are not so easy and Ohtsuki [9] gave a proof for 5_2 knot by using the Poisson sum formula adding to the saddle point method used in Kashaev's paper [4] where he discovered the relation between certain quantum invariants and the hyperbolic volume of the knot complement. Then Ohtsuki-Yokota [11] gave proofs for prime six crossings knots, Ohtsuki [10] gave proofs for prime seven crossings knots. For prime knots with larger crossing numbers, the volume conjecture has not been proved yet. Recently, Chen-Zhu [2] announced a proof of the volume conjecture for an infinite family of twist knots, but not for all twist knots. A twist knot is the $(2, s)$ double twist knot for some integer s.

Here, we show the following.

Theorem 1. *Let K be a hyperbolic (s, t) ndouble twist knot or link K given in Figure 1. Then we have*

$$2\,\pi \lim_{N\to\infty} \frac{|J_{N-1}(K)|}{N} = \mathrm{Vol}(S^3 \setminus K).$$

To prove this theorem, we first investigate the eigenvalues of the representation matrices of some elements of the fundamental group $\pi_1(S^3 \setminus K)$. Then compare these eigenvalues with the parameters at the saddle point of the volume potential function constructed from the colored Jones polynomial. At the end, we show that the value of the volume potential function at the saddle point coincides with the complex volume $\mathrm{Vol}(S^3 \setminus K) + \sqrt{-1}\,\mathrm{CS}(S^3 \setminus K)$ by comparing with the Neumann-Zagier function. Here we use the fact that the double twist knot or link is obtained by surgeries along two components of the Borromean rings and its variations as in Figure 2.

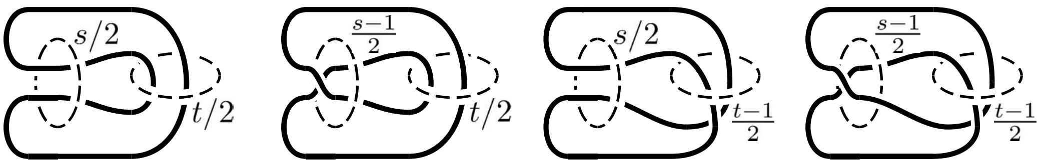

Figure 2: Surgery presentation of double twist knots and links.

2 Representation of the knot group

Before introducing the complexified tetrahedron, we investigate the geometric $\mathrm{SL}(2, \mathbb{C})$ representation of the complement of a double twist knot K. We assign the elements g_1, $\cdots$, g_4, g_{12}, g_{23} of $\pi_1(S^3 \setminus K)$ as in Figure 3. Then these elements satisfy the following relations.

$$g_{12} = g_1 g_2, \quad g_{23} = g_2 g_3, \quad g_1 g_2 g_3 g_4 = 1, \tag{1}$$

$$\begin{cases} g_1^{-1} = {g_{23}}^{\frac{s}{2}} g_2 {g_{23}}^{-\frac{s}{2}} \\ g_4^{-1} = {g_{23}}^{\frac{s}{2}} g_3 {g_{23}}^{-\frac{s}{2}} \end{cases} \text{if } s \text{ is even,} \quad \begin{cases} g_1^{-1} = {g_{23}}^{\frac{s+1}{2}} g_3 {g_{23}}^{-\frac{s+1}{2}} \\ g_4^{-1} = {g_{23}}^{\frac{s-1}{2}} g_2 {g_{23}}^{-\frac{s-1}{2}} \end{cases} \text{if } s \text{ is odd,} \tag{2}$$

$$\begin{cases} g_4^{-1} = {g_{12}}^{\frac{t}{2}} g_1 {g_{12}}^{-\frac{t}{2}} \\ g_3^{-1} = {g_{12}}^{\frac{t}{2}} g_2 {g_{12}}^{-\frac{t}{2}} \end{cases} \text{if } t \text{ is even,} \quad \begin{cases} g_4^{-1} = {g_{12}}^{\frac{t+1}{2}} g_2 {g_{12}}^{-\frac{t+1}{2}} \\ g_3^{-1} = {g_{12}}^{\frac{t-1}{2}} g_1 {g_{12}}^{-\frac{t-1}{2}} \end{cases} \text{if } t \text{ is odd.} \tag{3}$$

(s,t) double twist knot K : 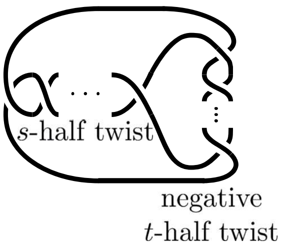

Elements of $\pi_1(S^3 \setminus K)$: 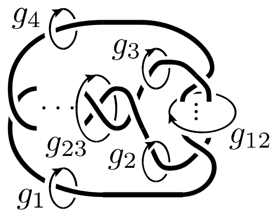

Figure 3: Elements g_1, g_2, g_3, g_4, g_{12}, g_{23} in $\pi_1(S^3 \setminus K)$.

The following matrices give the geometric $\mathrm{SL}(2,\mathbb{C})$ representation $\rho : \pi_1(S^3 \setminus K) \to \mathrm{SL}(2,\mathbb{C})$ where g_1, g_2, g_3, g_4 are mapped to parabolic matrices with eigenvalues -1, g_{23} is mapped to the diagonal matrix $\rho(g_{23}) = \begin{pmatrix} u^{-1} & 0 \\ 0 & u \end{pmatrix}$, and the eigenvalues of $\rho(g_{12})$ are v and v^{-1}. Then the relations $g_1 g_2 = g_{12}$, $g_2 g_3 = g_{23}$, $g_1 g_2 g_3 g_4 = 1$ imply that the following representation.

$$\rho(g_1) = \begin{pmatrix} -\frac{2u}{u+1} & \frac{u-1}{u+1} \\ -\frac{u-1}{u+1} & -\frac{2}{u+1} \end{pmatrix},$$

$$\rho(g_2) = \begin{pmatrix} -\frac{2}{u+1} & -\frac{(u+1)^2(v^2+1)-8uv+(u+1)(v-1)\sqrt{D}}{2v(u-1)(u+1)} \\ \frac{(u+1)^2(v^2+1)-8uv-(u+1)(v-1)\sqrt{D}}{2v(u-1)(u+1)} & -\frac{2u}{u+1} \end{pmatrix},$$

$$\rho(g_3) = \begin{pmatrix} -\frac{2}{u+1} & u\frac{(u+1)^2(v^2+1)-8uv+(u+1)(v-1)\sqrt{D}}{2v(u-1)(u+1)} \\ -\frac{(u+1)^2(v^2+1)-8uv-(u+1)(v-1)\sqrt{D}}{2uv(u-1)(u+1)} & -\frac{2u}{u+1} \end{pmatrix},$$

$$\rho(g_4) = \begin{pmatrix} -\frac{2u}{u+1} & -\frac{u(u-1)}{u+1} \\ \frac{u-1}{u(u+1)} & -\frac{2}{u+1} \end{pmatrix}, \qquad \text{where } D = (u+1)^2(v+1)^2 - 16uv.$$

The elements of $\mathrm{SL}(2,\mathbb{C})$ acts on $\mathbb{C} = \partial\mathbb{H}^3$ by the linear fractional transformation, and the fixed points p_1, p_2, p_3, p_4 of $\rho(g_1)$, $\rho(g_2)$, $\rho(g_3)$, $\rho(g_4)$ by this action are as follows.

$$p_1 = 1, \qquad p_2 = \frac{(u+1)^2(v^2+1) - 8uv + (u+1)(v-1)\sqrt{D}}{2v(u-1)^2},$$

$$p_3 = -u\frac{(u+1)^2(v^2+1) - 8uv - (u+1)(v-1)\sqrt{D}}{2v(u-1)^2}, \qquad p_4 = -u.$$

The fixed points of $\rho(g_{23})$ are 0 and ∞, and the fixed points of $\rho(g_{12})$ are

$$-\frac{(u+1)^2(v+1) - 8u + (u+1)\sqrt{D}}{4(u-1)}, \qquad -\frac{(u+1)^2(v+1) - 8uv - (u+1)\sqrt{D}}{4(u-1)v}.$$

Let ρ' be the representation similar to ρ where g_{12} is mapped to the diagonal matrix $\rho'(g_{12}) = \begin{pmatrix} v^{-1} & 0 \\ 0 & v \end{pmatrix}$ instead of g_{23}. Such ρ' is obtained by the transformation matrix

$$Q = \begin{pmatrix} -\frac{(u+1)^2(v+1)-8u+(u+1)\sqrt{D}}{4(u-1)} & -\frac{(u+1)(v+1)(u+v)-8uv+(uv-1)\sqrt{D}}{2(u-1)(v-1)} \\ 1 & \frac{(u+1)(v+1)^2-8v+(v+1)\sqrt{D}}{4(v-1)} \end{pmatrix}.$$

For $g \in \pi_1(S^3 \setminus K)$, let $\rho'(g) = Q^{-1}\,\rho(g)\,Q$, then we have

$$\rho'(g_1) = \begin{pmatrix} -\frac{2}{v+1} & -\frac{v-1}{v+1} \\ \frac{v-1}{v+1} & -\frac{2v}{v+1} \end{pmatrix}, \qquad \rho'(g_2) = \begin{pmatrix} -\frac{2}{v+1} & \frac{v-1}{v(v+1)} \\ -\frac{v(v-1)}{v+1} & -\frac{2v}{v+1} \end{pmatrix},$$

$$\rho'(g_3) = \begin{pmatrix} -\frac{2v}{v+1} & -v\frac{\left((u^2+1)(v+1)^2-8uv+(u-1)(v+1)\sqrt{D}\right)}{2u(v-1)(v+1)} \\ \frac{(u^2+1)(v+1)^2-8uv-(u-1)(v+1)\sqrt{D}}{2u(v-1)(v+1)} & -\frac{2}{v+1} \end{pmatrix},$$

$$\rho'(g_4) = \begin{pmatrix} -\frac{2v}{v+1} & \frac{\left((u^2+1)(v+1)^2-8uv+(u-1)(v+1)\sqrt{D}\right)}{2u(v-1)(v+1)} \\ -\frac{(u^2+1)(v+1)^2-8uv-(u-1)(v+1)\sqrt{D}}{2uv(v-1)(v+1)} & -\frac{2}{v+1} \end{pmatrix}.$$

The fixed points q_1, q_2, q_3, q_4 of $\rho'(g_1)$, $\rho'(g_2)$, $\rho'(g_3)$, $\rho'(g_4)$ on $\partial\mathbb{H}^3$ are

$$q_1 = 1, \qquad q_2 = -v, \qquad q_3 = -v\frac{(u^2+1)(v+1)^2 - 8uv + (u-1)(v+1)\sqrt{D}}{2u(v-1)^2},$$
$$q_4 = \frac{(u^2+1)(v+1)^2 - 8uv + (u-1)(v+1)\sqrt{D}}{2u(v-1)^2}.$$

The fixed points of $\rho'(g_{12})$ are 0 and ∞, and the fixed points of $\rho'(g_{23})$ are

$$-\frac{(u^2+1)(v+1)^2 - 8v + (v+1)\sqrt{D}}{4(v-1)}, \qquad -\frac{(u^2+1)(v+1)^2 - 8uv - (v+1)\sqrt{D}}{4u(v-1)}.$$

The relations (2) and (3) imply that the eigenvalues u and v are determined by

$$(-u)^s = p_2, \qquad (-v)^{-t} = q_4. \tag{4}$$

Moreover, the geometric representation is given by the solution among the solutions of (4) satisfying

$$s\log(-u) + \log p_2^{-1} = \pm 2\pi\sqrt{-1}, \qquad -t\log(-v) + \log q_4^{-1} = \pm 2\pi\sqrt{-1}. \tag{5}$$

3 Complexified tetrahedron

In the previous section, we introduced the eigenvalues u and v of $\rho(g_{23})$ and $\rho(g_{12})$. Here we give a geometric interpretation of these values. To do this, we introduce the complexified tetrahedron.

Before introducing the complexified tetrahedron, we recall generalized tetrahedron, which is determined by four planes in general position in the hyperbolic space. In the hyperbolic space, two or three planes sometimes do not intersect even if they are in general position, but we can consider some geometric object as in Figure 4. For example, if two plane do not intersect, then the edge corresponding to these planes is the common perpendicular line segment. The edges of such tetrahedrons are parametrized by dihedral

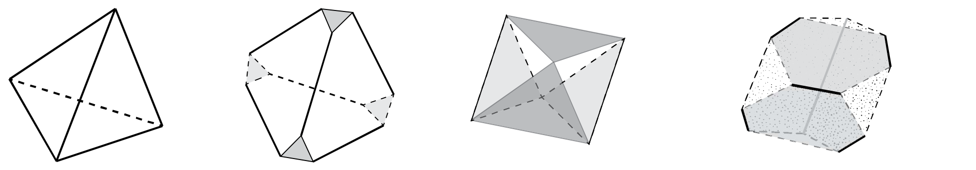

Figure 4: Generalized tetrahedrons in the hyperbolic space.

angles and lengths, and it is natural to consider the angle as a purely imaginal number and the length as a real number. Here we generalize these parameters of generalized tetrahedrons to actual complex numbers as in Figure 5. The length ℓ is generalized to

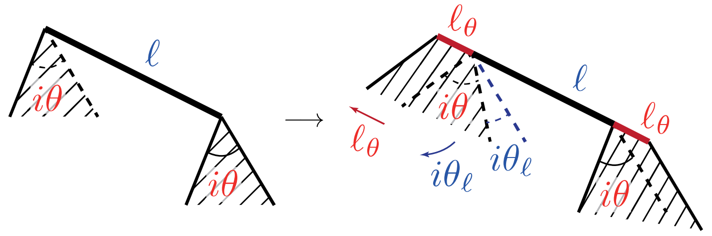

Figure 5: Complexification of the dihedral angle and the edge length.

$\ell + i\,\theta_\ell$ and $i\,\theta$ is generalized to $i\,\theta + \ell_\theta$.

Let B be the Borromean rings. The double twist knot is obtained by surgeries along two components of B as in Figure 2. The complement of B has a hyperbolic structure, and is divided into two copies of the regular ideal octahedron in Figure 4, which is one of the extremal generalized tetrahedron. In other words, glueing two copies of the regular ideal octahedron is a fundamental domain of the action of $\pi_1(S^3 \setminus B)$ to the hyperbolic space $\mathbb{H}^3$. The six vertices of the octahedron corresponds to the edges of a tetrahedron, and its edge lengths and dihedral angles are all zero. The six vertices correspond to the fixed points of parabolic elements of $SL(2, \mathbb{C})$ representing g_1, g_2, g_3, g_4, g_{12}, g_{23} of $\pi_1(S^3 \setminus B)$. For a double twist knot K, the hyperbolic structure of its complement is obtained as a deformation of the complement of B. For $\pi_1(S^3 \setminus K)$, the matrices for g_1, g_2, g_3, g_4 are parabolic, and the matrices for g_{12}, g_{23} are deformed to a generic matrices. Actual representations of these matrices are given in the previous section.

Now we look at the fundamental domain of the action of $\pi_1(S^3 \setminus K)$ which is obtained by a deformation of the regular ideal octahedron. The regular ideal octahedron has six vertices, and we deform a pair of opposite two vertices. Other four vertices are fixed points p_1, p_2, p_3, p_4 of g_1, g_2, g_3, g_4. The elements g_{23}, g_{12} have axes l_{23}, l_{12}, so we assign

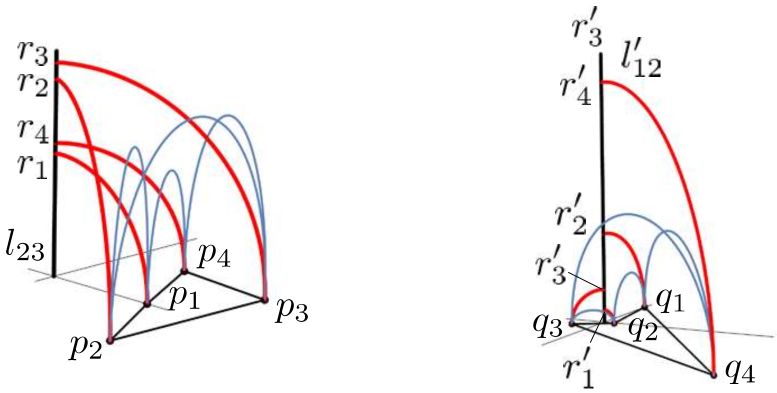

representation ρ representation ρ'

Figure 6: Complexified tetrahedron. The left explains the upper part and the right explains the lower part. These two are glued at blue lines and p_i and q_i are identified.

complex parameters to these axes u, v, which is the eigenvalues of g_{23}, g_{12}. Let r_1, r_2, r_3, r_4 be the foots of perpendicular on l_{23} from p_1, p_2, p_3, p_4, and, r'_1, r'_2, r'_3, r'_4 be the foots of perpendicular on l_{12} from p_1, p_2, p_3, p_4. Let us define eight faces $p_1p_2r_2r_1$, $p_2p_3r_3r_2$, $p_3p_4r_4r_3$, $p_4p_1r_1r_4$, $p_1p_2r'_2r'_1$, $p_2p_3r'_3r'_2$, $p_3p_4r'_4r'_3$, $p_4p_1r'_1r'_4$. These faces are not flat and are not defined uniquely, but the edges of the faces are straight lines and we define these faces topologically. Let T be the subset of $\mathbb{H}^3$ surrounded by these eight faces, and here we call T *a complexified tetrahedron* corresponding to the double twist. Let T' be similar complexified tetrahedron constructed from $(-u)p_1$, $(-u)p_2$, $(-u)p_3$, $(-u)p_4$, $(-u)l_{12}$ and $(-u)l_{23} = l_{23}$. Then T and T' are adjacent at the face $p_3p_4r_4r_3$ and $T \cup T'$ is a fundamental domain of the action of $\pi_1(S^3 \setminus K)$ to $\mathbb{H}^3$.

Let K be the $(6, 2)$ double twist knot, which is the twist knot 8_1 in Rolfsen's table. Then the eigenvalues u, v satisfying (4) and (5) where the sums are both $+2\pi i$ is

$$u = -0.619307 - 0.884567i, \qquad v = 1.72565 + 2.06055i,$$

and from these u, v, we get the complex numbers $p_1, \cdots, p_4, p_1, \cdots, q_4$ as follows.

$$\begin{aligned} p_1 &= 1, & p_2 &= 1.3731 - 0.7921i, & p_3 &= 1.5511 + 0.7240i, & p_4 &= 0.6193 + 0.8845i, \\ q_1 &= 1, & q_2 &= -1.7256 - 2.0605i, & q_3 &= -0.2388 + 0.2852i, & q_4 &= -0.0242 - 0.1362i, \end{aligned}$$

Now take foots of perpendicular from p_i to l_{23}, we get pictures as in Figure 6. The blue lines correspond to the four edges representing the equator of the octahedron. The left picture explains the upper part and the right picture explains the lower part of the complexified tetrahedron. The line l_{23} is the axis of the action of g_{23} and the multiplication by the eigenvalue u of t_{23} maps p_2, p_3 to p_1, p_4. The action of $\rho(g_{23})$ on $\partial\mathbb{H}^3$ corresponds to the multiplication of u^2, so we get the picture in Figure 7. Similarly, the action of $\rho'(g_{12})$ corresponds to the multiplication of v^{-2} and is also explained the figure.

Observation 1. The complexified tetrahedron described above is a deformation of the regular ideal octahedron associated with the Borromean rings complement. As a generalized

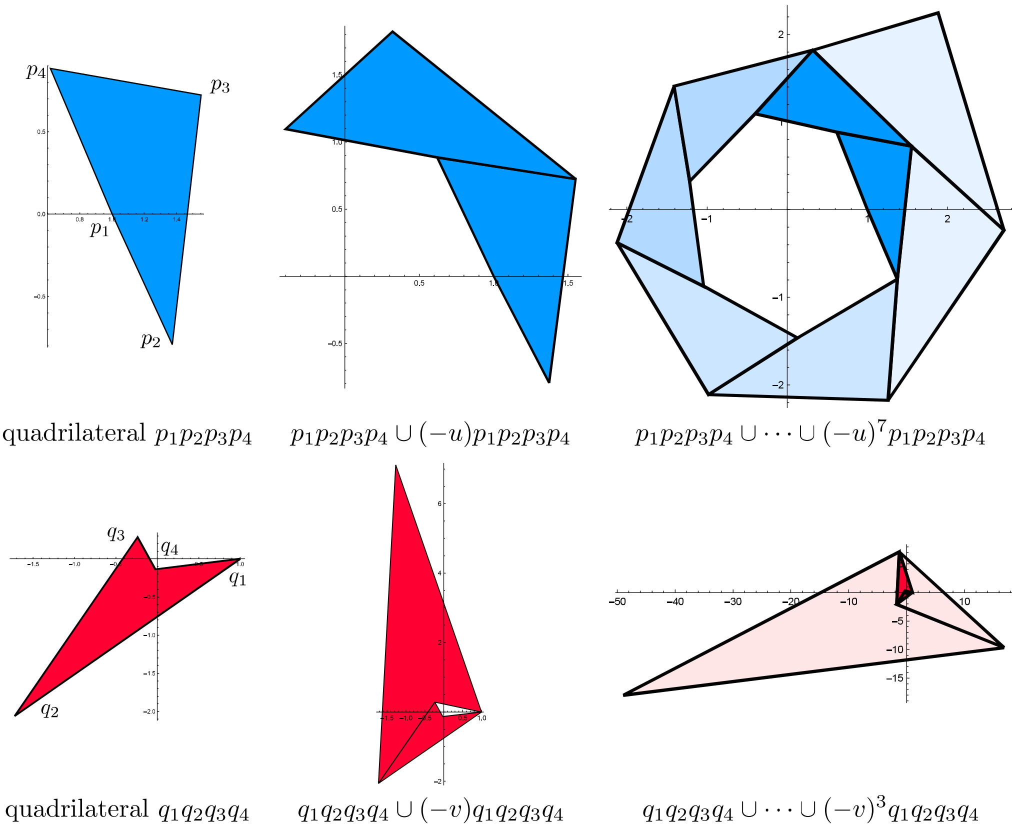

Figure 7: The actions of g_{23} and g_{12}. The upper row is for the action of $\rho(g_{23})$ and the lower row is for the action of $\rho'(g_{12})$. They act $\partial\mathbb{H}^3$ by rotations and shrinking/enlargement around the origin. The middle pictures correspond to the fundamental domain of the action of $\pi_1(S^3 \setminus K)$.

tetrahedron, the six edges of the tetrahedron correspond to the six vertices of the regular ideal octahedron, and these edges are parametrized by all zero for the angles and lengths. For the complexified tetrahedron associated to the double twist knot complement, one edge has $\log u = \log p_4$ as the angle parameter and the opposite edge has $\log v = \log q_2$ as the angle parameter. Moreover, $\log p_2$ coincides with the length parameter of the first edge, and $\log q_4$ coincides with the length parameter of the second edge. For other edges, parameters are all zero and they correspond to ideal points on $\partial\mathbb{H}^3$. See Figure 8.

Note that the signature of angles and lengths are not canonically determined. For example, as length parameters, we may choose $-\log p_2$, $-\log q_4$ instead of $\log p_2$, $\log q_4$.

4 Colored Jones polynomial and ADO invariant

Let N be an odd integer greater than equal to three. The colored Jones invariant $J_{N-1}(K)$ of a knot K at $q = e^{\frac{\pi i}{N}}$ is equal the ADO invariant $\mathrm{AKO}_N(K^{\frac{N-1}{2}})$ introduced in [1], where K is colored by $\frac{N-1}{2}$. Here we use the following notations.

$$q^a = \exp\frac{\pi i a}{N} \quad (a \in \mathbb{C}), \quad \{a\} = q^a - q^{-a}, \quad \{n\}! = \{n\}\{n-1\}\dots\{1\},$$

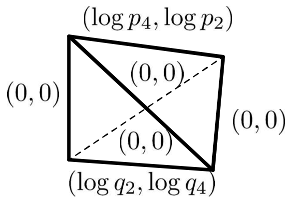

(a, b) means that a is the angle parameter and b is the length parameter. The top edge is parametrized by $(\log p_4, \log p_2)$, the bottom edge is parametrized by $(\log q_2, \log q_4)$, and the other edges are parametrized by $(0, 0)$.

Figure 8: Parametrization for the complexified tetrahedron associated to the double twist knot.

$$\{a,k\} = \{a\}\{a-1\}\dots\{a-k+1\}, \qquad \begin{bmatrix} a \\ b \end{bmatrix} = \frac{\{a, a-b\}}{\{a-b\}!} \quad (a-b \in \{0,1,\dots,N-1\}),$$
$$r_a = a(a+1-N) = (a - \tfrac{N-1}{2})^2 - \tfrac{(N-1)^2}{4}.$$

The ADO invariant is generalized to colored knotted graphs in [3] whose colors are in $(\mathbb{C} \setminus \mathbb{Z}/2) \cup (N\mathbb{Z}-1)/2$, and it satisfies the following properties.

ADO_N (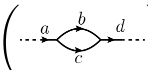) $= \delta_{ad} \begin{bmatrix} 2a+N \\ 2a+1 \end{bmatrix}$ ADO_N (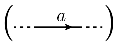),

ADO_N (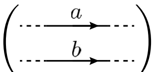) $= \displaystyle\sum_{a+b-c=0,1,\cdots,N-1} \begin{bmatrix} 2c+N \\ 2c+1 \end{bmatrix}^{-1}$ ADO_N (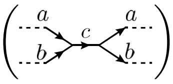),

ADO_N (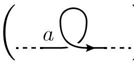) $= q^{2r_a}$ ADO_N (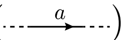),

ADO_N (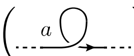) $= q^{-2r_a}$ ADO_N (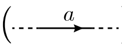),

ADO_N (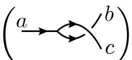) $= q^{r_a - r_b - r_c}$ ADO_N (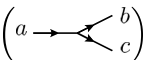),

ADO_N (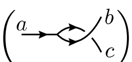) $= q^{-(t_a - t_b - t_c)}$ ADO_N (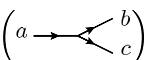),

ADO_N (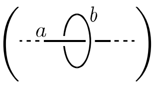) $= i^{N-1}\,\{2a+N, N-1\}\, q^{(2a+1-N)(2b+1-N)}$ ADO_N (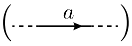),

ADO_N (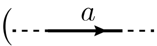) $=$ ADO_N (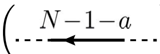) (dual representation).

The ADO invariant of the colored tetrahedral graph is a version of the quantum $6j$ symbol and is given in [3] as follows. $\mathrm{ADO}_N(K)$ is computed formally as follows.

$$\begin{Bmatrix} a & b & e \\ d & c & f \end{Bmatrix}_q = \mathrm{ADO}_N$$ (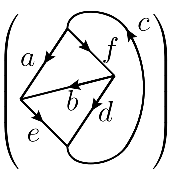)

Figure 9: The quantum $6j$ symbol defined by the colored tetrahedral graph.

$$\begin{Bmatrix} a & b & e \\ d & c & f \end{Bmatrix}_q = (-1)^{N-1} \frac{\{B_{dec}\}!\{B_{abe}\}!}{\{B_{bdf}\}!\{B_{afc}\}!} \begin{bmatrix} 2e \\ A_{abe}+1-N \end{bmatrix} \begin{bmatrix} 2e \\ B_{ced} \end{bmatrix}^{-1} \times$$
$$\sum_{m=\max(0,-B_{bdf}+B_{dec})}^{\min(B_{dec},B_{afc})} \begin{bmatrix} A_{acf}+1-N \\ 2c+m+1-N \end{bmatrix} \begin{bmatrix} B_{acf}+m \\ B_{acf} \end{bmatrix} \begin{bmatrix} B_{bfd}+B_{dec}-m \\ B_{bfd} \end{bmatrix} \begin{bmatrix} B_{cde}+m \\ B_{dfb} \end{bmatrix}.$$

where

$$A_{xyz} = x+y+z, \qquad B_{xyz} = x+y-z.$$

Since

$$\mathrm{ADO}_N\left(\right.$$
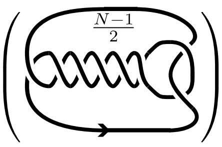

$$\left.\right) = \sum_{k,l=0}^{N-1} \begin{bmatrix} 2k+N \\ 2k+1 \end{bmatrix}^{-1} \begin{bmatrix} 2l+N \\ 2l+1 \end{bmatrix}^{-1} \mathrm{ADO}_N\left(\right.$$
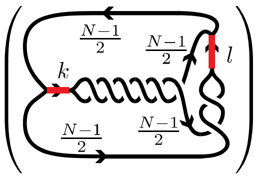

$$\left.\right),$$

$(s,t) = (6,2)$ case

$\mathrm{ADO}_N(K^{\frac{N-1}{2}})$ is computed as follows.

$$\mathrm{ADO}_N(K^{\frac{N-1}{2}}) =$$
$$(-1)^{N-1} \sum_{k,l=0}^{N-1} \frac{q^{s(k-\frac{N-1}{2})^2 - t(l-\frac{N-1}{2})^2 + (s-t)\frac{(N-1)^2}{4}} \{N-1\}!^2}{\{2k+N, N-1\}\{2l+N, N-1\}} \begin{Bmatrix} \frac{N-1}{2} & \frac{N-1}{2} & l \\ \frac{N-1}{2} & \frac{N-1}{2} & k \end{Bmatrix}_q$$
$$= q^{(s-t)\frac{(N-1)^2}{4}} N^2 \sum_{k,l=0}^{N-1} \frac{\{2k+1\}\{2l+1\} q^{s(k-\frac{N-1}{2})^2 - t(l-\frac{N-1}{2})^2}}{\{2l+N, N\}\{2k+N, N\}} \begin{Bmatrix} \frac{N-1}{2} & \frac{N-1}{2} & l \\ \frac{N-1}{2} & \frac{N-1}{2} & k \end{Bmatrix}_q.$$

To tell the truth, this computation is wrong since the color k, l is in $\mathbb{Z}$. However, we can perturb the color by ε, δ and obtain $\mathrm{ADO}_N(K^{\frac{N-1}{2}})$ as the limit $\varepsilon \to 0$ and $\delta \to 0$ as follows.

$$\mathrm{ADO}_N(K^{\frac{N-1}{2}}) = \lim_{\varepsilon,\delta\to 0} \mathrm{ADO}_N\left(\right.$$
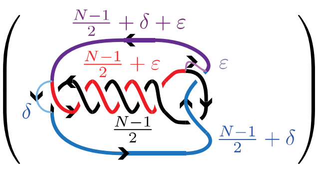

$$\left.\right) =$$

$$\lim_{\varepsilon,\delta\to 0} \sum_{k,l=0}^{N-1} \begin{bmatrix} 2k+2\varepsilon+N \\ 2k+2\varepsilon+1 \end{bmatrix}^{-1} \begin{bmatrix} 2l+2\delta+N \\ 2l+2\delta+1 \end{bmatrix}^{-1} \times$$
$$q^{sr_{k+\varepsilon} - sr_{(N-1)/2+\varepsilon} - tr_{l+\delta} + tr_{(N-1)/2+\delta} + (s-t)(N-1)^2/4} \mathrm{ADO}_N\left(\right.$$
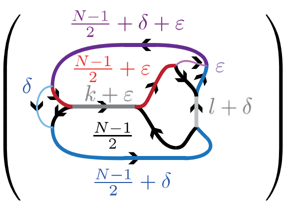

$$\left.\right)$$

$$= \lim_{\varepsilon,\delta\to 0} N^2 \sum_{k,l=0}^{N-1} \frac{\{2k+2\varepsilon+1\}\{2l+2\delta+1\} q^{sr_{k+\varepsilon} - sr_{(N-1)/2+\varepsilon} - tr_{l+\delta} + tr_{(N-1)/2+\delta} + (s-t)(N-1)^2/4}}{\{2k+2\varepsilon+N, N\}\{2l+2\delta+N, N\}} \times$$

$$
\begin{Bmatrix} \frac{N-1}{2}+\delta & \frac{N-1}{2} & l+\delta \\ \frac{N-1}{2}+\varepsilon & \frac{N-1}{2}+\varepsilon+\delta & k+\varepsilon \end{Bmatrix}_q
$$

$$
= \lim_{\varepsilon,\delta\to 0} \frac{N^2\, q^{(s-t)(N-1)^2/4}}{\{2\varepsilon+N,N\}\{2\delta+N,N\}} \sum_{k,l=0}^{N-1} \{2k+2\varepsilon+1\}\{2l+2\delta+1\}\times
$$

$$
q^{sr_{k+\varepsilon}-sr_{(N-1)/2+\varepsilon}-tr_{l+\delta}+tr_{(N-1)/2+\delta}} \begin{Bmatrix} \frac{N-1}{2}+\delta & \frac{N-1}{2} & l+\delta \\ \frac{N-1}{2}+\varepsilon & \frac{N-1}{2}+\varepsilon+\delta & k+\varepsilon \end{Bmatrix}_q .
$$

Now we use L'Hoptal's rule. The actual computation shows that

$$
\begin{aligned}
\frac{\partial}{\partial\varepsilon} \begin{Bmatrix} \frac{N-1}{2}+\delta & \frac{N-1}{2} & l+\delta \\ \frac{N-1}{2}+\varepsilon & \frac{N-1}{2}+\varepsilon+\delta & k+\varepsilon \end{Bmatrix}_q \Bigg|_{\varepsilon=0} &= \frac{\partial}{\partial\varepsilon} \begin{Bmatrix} \frac{N-1}{2}+\delta & \frac{N-1}{2} & l+\delta \\ \frac{N-1}{2} & \frac{N-1}{2}+\delta & k+\varepsilon \end{Bmatrix}_q \Bigg|_{\varepsilon=0} \\
&= \frac{\partial}{\partial x} \begin{Bmatrix} \frac{N-1}{2}+\delta & \frac{N-1}{2} & l+\delta \\ \frac{N-1}{2} & \frac{N-1}{2}+\delta & x \end{Bmatrix}_q \Bigg|_{x=k},
\end{aligned}
$$

$$
\begin{aligned}
\frac{\partial}{\partial\delta} \begin{Bmatrix} \frac{N-1}{2}+\delta & \frac{N-1}{2} & l+\delta \\ \frac{N-1}{2}+\varepsilon & \frac{N-1}{2}+\varepsilon+\delta & k+\varepsilon \end{Bmatrix}_q \Bigg|_{\delta=0} &= \frac{\partial}{\partial\delta} \begin{Bmatrix} \frac{N-1}{2} & \frac{N-1}{2} & l+\delta \\ \frac{N-1}{2}+\varepsilon & \frac{N-1}{2}+\varepsilon & k+\varepsilon \end{Bmatrix}_q \Bigg|_{\delta=0} \\
&= \frac{\partial}{\partial y} \begin{Bmatrix} \frac{N-1}{2} & \frac{N-1}{2} & y \\ \frac{N-1}{2}+\varepsilon & \frac{N-1}{2}+\varepsilon & k+\varepsilon \end{Bmatrix}_q \Bigg|_{y=l},
\end{aligned}
$$

$$
\begin{aligned}
\frac{\partial^2}{\partial\varepsilon\partial\delta} \begin{Bmatrix} \frac{N-1}{2}+\delta & \frac{N-1}{2} & l+\delta \\ \frac{N-1}{2}+\varepsilon & \frac{N-1}{2}+\varepsilon+\delta & k+\varepsilon \end{Bmatrix}_q \Bigg|_{\varepsilon=\delta=0} &= \frac{\partial^2}{\partial\varepsilon\partial\delta} \begin{Bmatrix} \frac{N-1}{2} & \frac{N-1}{2} & l+\delta \\ \frac{N-1}{2} & \frac{N-1}{2} & k+\varepsilon \end{Bmatrix}_q \Bigg|_{\varepsilon=\delta=0} \\
&= \frac{\partial^2}{\partial x\partial y} \begin{Bmatrix} \frac{N-1}{2} & \frac{N-1}{2} & y \\ \frac{N-1}{2}+\varepsilon & \frac{N-1}{2}+\varepsilon & x \end{Bmatrix}_q \Bigg|_{x=k,y=l}.
\end{aligned}
$$

Therefore, we have

$$
\begin{aligned}
&\mathrm{ADO}_N(K^{\frac{N-1}{2}}) = N\, q^{(s-t)(N-1)^2/4}\times \\
&\qquad \frac{\displaystyle\sum_{k,l=0}^{N-1} \frac{\partial^2}{\partial x\partial y}\{2x+1\}\{2y+1\} q^{s(x-(N-1)/2)^2-t(y-(N-1)/2)^2} \begin{Bmatrix} \frac{N-1}{2} & \frac{N-1}{2} & y \\ \frac{N-1}{2} & \frac{N-1}{2} & x \end{Bmatrix}_q \Bigg|_{x=k,y=l}}{\displaystyle\frac{\partial^2}{\partial\varepsilon\partial\delta}\{2\varepsilon+N,N\}\{2\delta+N,N\}\Bigg|_{\varepsilon=\delta=0}} \\
&= (-1)^N \frac{N}{16\pi^2}\, q^{(s-t)(N-1)^2/4}\times \\
&\qquad \sum_{k,l=0}^{N-1} \frac{\partial^2}{\partial x\partial y}\{2x+1\}\{2y+1\} q^{s(x-(N-1)/2)^2-t(y-(N-1)/2)^2} \begin{Bmatrix} \frac{N-1}{2} & \frac{N-1}{2} & y \\ \frac{N-1}{2} & \frac{N-1}{2} & x \end{Bmatrix}_q \Bigg|_{x=k,y=l}.
\end{aligned}
$$

So, to investigate the limit

$$
2\,\pi \lim_{N\to\infty} \frac{|\,\mathrm{ADO}(K^{\frac{N-1}{2}})|}{N}, \tag{6}
$$

it is enough to see the part

$$\sum_{k,l=0}^{N-1} \frac{\partial^2}{\partial x \partial y} \{2x+1\}\{2y+1\} q^{s(x-(N-1)/2)^2 - t(y-(N-1)/2)^2} \begin{Bmatrix} \frac{N-1}{2} & \frac{N-1}{2} & y \\ \frac{N-1}{2} & \frac{N-1}{2} & x \end{Bmatrix}_q \Bigg|_{x=k, l=y} . \tag{7}$$

5 Saddle points and big cancellation

To investigate (7), we apply the Poisson sum formula and then the saddle point method. We first rewrite (7) by an analytic funtion. There is an analytic functions $\Phi_N(x,y)$ and $\Phi(x,y)$ such that

$$e^{\frac{N}{2\pi i}\Phi_N(2\pi\frac{2k+1}{2N}, 2\pi\frac{2l+1}{2N})} = \begin{Bmatrix} \frac{N-1}{2} & \frac{N-1}{2} & l \\ \frac{N-1}{2} & \frac{N-1}{2} & k \end{Bmatrix}_q , \qquad \Phi_N(x,y) \underset{N\to\infty}{\longrightarrow} \Phi(x,y).$$

Note that

$$\begin{Bmatrix} \frac{N-1}{2} & \frac{N-1}{2} & l \\ \frac{N-1}{2} & \frac{N-1}{2} & k \end{Bmatrix}_q = \sum_{m=\max(k,l)}^{\min(k+l,N-1)} \frac{\{m\}!^2}{\{m-k\}!^2\,\{m-l\}!^2\,\{k+l-m\}!^2}$$

and

$$\begin{aligned} \log \frac{\{m\}!^2}{\{m-k\}!^2\,\{m-l\}!^2\,\{k+l-m\}!^2} &\underset{N\to\infty}{\sim} \\ &\frac{N}{2\pi}\Big((iz)^2 - 2(ix+iy)iz + (ix)^2 + (ix)(iy) + (iy)^2 - \\ &\qquad 2\mathrm{Li}_2\left(e^{iz}\right) + 2\mathrm{Li}_2\left(e^{i(z-x)}\right) + 2\mathrm{Li}_2\left(e^{i(z-y)}\right) + 2\mathrm{Li}_2\left(e^{i(x-y-z)}\right)\Big) \end{aligned}$$

for $x = 2\pi\frac{2k+1}{N}$, $y = 2\pi\frac{2l+1}{N}$, $z = 2\pi\frac{2m+1}{N}$. Let

$$\begin{aligned} \varphi(x,y,z) = (iz)^2 - 2(ix+iy)iz + (ix)^2 + (ix)(iy) + (iy)^2 - \\ 2\mathrm{Li}_2\left(e^{iz}\right) + 2\mathrm{Li}_2\left(e^{i(z-x)}\right) + 2\mathrm{Li}_2\left(e^{i(z-y)}\right) + 2\mathrm{Li}_2\left(e^{i(x-y-z)}\right). \end{aligned}$$

Then, for $x, y \in [0, 2\pi]$, we have

$$\sum_{m=\max(k,l)}^{\min(k+l,N-1)} \frac{\{m\}!^2}{\{m-k\}!^2\,\{m-l\}!^2\,\{k+l-m\}!^2} \underset{N\to\infty}{\sim} \exp\left(\frac{N}{2\pi}\varphi(x,y,z_0)\right)$$

where z_0 satisfies

$$\frac{\partial}{\partial z}\varphi(x,y,z) = 0, \tag{8}$$

and it corresponds to the maximal value among $z \in [0, 2\pi]$. By relacing $\xi = e^{ix}$, $\zeta = e^{iy}$, $\eta = e^{iz}$, the equation (8) is equivalent to the quadratic equation

$$2\eta^2 - (\xi+1)(\zeta+1)\eta + 2\xi\zeta = 0,$$

and the solutions are given by

$$\eta = \frac{1}{4}\xi^{1/2}\zeta^{1/2}\left((\xi^{1/2}+\xi^{-1/2})(\zeta^{1/2}+\zeta^{-1/2}) \pm \sqrt{(\xi^{1/2}+\xi^{-1/2})^2(\zeta^{1/2}+\zeta^{-1/2})^2-16}\right).$$

These solutions are both sit on the unit circle and the solution corresponds to the maximal value is

$$\eta_0 = \frac{1}{4}\xi^{1/2}\zeta^{1/2}\left((\xi^{1/2}+\xi^{-1/2})(\zeta^{1/2}+\zeta^{-1/2}) + i\sqrt{16-(\xi^{1/2}+\xi^{-1/2})^2(\zeta^{1/2}+\zeta^{-1/2})^2}\right),$$

and $z_0 = \frac{1}{i}\log\eta_0$. Let $\Phi(x,y) = \varphi(x,y,z_0)$,

$$\Psi_N^{\varepsilon_1,\varepsilon_2}(2\pi\tfrac{2\alpha+1}{2N}, 2\pi\tfrac{2\beta+1}{N}) =$$
$$\exp\left(\varepsilon_1\tfrac{2\alpha+1}{2N}\pi i + \varepsilon_2\tfrac{2\beta+1}{2N}\pi i + \tfrac{N}{2\pi i}\left(s(\tfrac{2\alpha+1-N}{2N}\pi i)^2 - t(\tfrac{2\beta+1-N}{2N}\pi i)^2 + \Phi_N(2\pi\tfrac{2\alpha+1}{2N}, 2\pi\tfrac{2\beta+1}{2N})\right)\right).$$

and

$$\Psi^{\varepsilon_1,\varepsilon_2}(2\pi\tfrac{2\alpha+1}{2N}, 2\pi\tfrac{2\beta+1}{N}) =$$
$$\exp\left(\varepsilon_1\tfrac{2\alpha+1}{2N}\pi i + \varepsilon_2\tfrac{2\beta+1}{2N}\pi i + \tfrac{N}{2\pi i}\left(s(\tfrac{2\alpha+1-N}{2N}\pi i)^2 - t(\tfrac{2\beta+1-N}{2N}\pi i)^2 + \Phi(2\pi\tfrac{2\alpha+1}{2N}, 2\pi\tfrac{2\beta+1}{2N})\right)\right).$$

Then

$$(7) \underset{N\to\infty}{\sim} \sum_{\varepsilon_1,\varepsilon_2=\pm1}\sum_{k,l=0}^{N-1} \varepsilon_1\varepsilon_2 \tfrac{\partial^2}{\partial\alpha\partial\beta}\ \Psi^{\varepsilon_1,\varepsilon_2}(2\pi\tfrac{2\alpha+1}{2N}, 2\pi\tfrac{2\beta+1}{N})\Big|_{\substack{\alpha=k\\ \beta=l}}. \tag{9}$$

The Poisson sum formula is the following identity which holds for rapidly decreasing function f.

$$\sum_{k\in\mathbb{Z}} f(k) = \sum_{m\in\mathbb{Z}} \widehat{f}(m), \quad \text{where } \widehat{f}(x) = \int_{\mathbb{R}} e^{-2\pi ixy} f(y)\,dy.$$

Applying this formula, we get the following.

$$\begin{aligned}|(7)| &\underset{N\to\infty}{\sim} \left|\sum_{\varepsilon_1,\varepsilon_2=\pm1}\sum_{m_1,m_2\in\mathbb{Z}} \varepsilon_1\varepsilon_2 \iint_{[0,2\pi]^2} e^{-Ni\left(m_1(x-\frac{\pi}{N})+m_2(y-\frac{\pi}{N})\right)} \tfrac{\partial^2}{\partial x\partial y}\Psi^{\varepsilon_1,\varepsilon_2}(x,y)\,dxdy\right| \\ &\underset{\text{integral by part}}{\sim} \left|\sum_{m_1,m_2\in\mathbb{Z}} m_1m_2 \iint_{[0,2\pi]^2} e^{\frac{N}{2\pi i}\left(2\pi(m_1x+m_2y)+s(x-\pi)^2-t(y-\pi)^2+\Phi(x,y)\right)}dxdy\right|.\end{aligned} \tag{10}$$

In this computation, $\sim$ means that there is an error, but this error is proved to be small enough and the limit (6) is obtained from the above formula.

Now we apply the saddle point method to (10). The equations to get the saddle points are the following.

$$\begin{aligned}&\frac{\partial}{\partial x}\left(2\pi(m_1x+m_2y)+s(x-\pi)^2-t(y-\pi)^2+\Phi(x,y)\right)=0,\\ &\frac{\partial}{\partial y}\left(2\pi(m_1x+m_2y)+s(x-\pi)^2-t(y-\pi)^2+\Phi(x,y)\right)=0.\end{aligned} \tag{11}$$

The largest contributing parts are $m_1 = \pm 1$, $m_2 = \pm 1$. Let (x_0, y_0) be a solution of these equations for $m_1 = m_2 = 1$, then we have the following.

Proposition 5.1. *The limit* (6) *coincides with the imaginary part*

$$\mathrm{Im}(2\pi(x_0 + y_0) + s(x_0 - \pi)^2 - t(y_0 - \pi)^2 + \Phi(x_0, y_0)). \tag{12}$$

To prove this, we have to check the condition so that we can apply the saddle point method for the integral (10). In this case, the range of sum for k and l are wide enough. It covers all over the unit circle of the complex plane. Moreover, the function Φ does not depend on s and t. The function Φ is based on the potential function of the colored Jones polynomial of the Borromean rings. Here we omit the proof for general case, and just explain for the $(6, 2)$ double twist knot.

The condition for applying the saddle point method is that the integral region fully surrounds the saddle point. We are now considering the function with two variables x and y. The integral region is two dimensional while the total space is $\mathbb{C}^2$ and is four dimensional. The saddle point is sit in this four dimensional space and the meaning of surrounding the saddle point is explained in Figure 10. In this case, the solution of the saddle point equation (11) for $m_1 = m_2 = 1$ is

$$x = 4.10158 - 0.0767893i, \qquad y = 0.873623 - 0.988685i,$$

while the integral region $[0, 2\pi]^2$ in $\mathbb{C}^2$. The saddle point is apart from the integral region, and we deform this region to the imaginary direction as in the figure so that it passes the saddle point, and the imaginary value is equal or less to the imaginary value at the saddle point . The contour for the imaginary part of the function $2\pi(x + y) + 6(x - \pi)^2 - 2(y - \pi)^2 + \Phi(x, y))$ looks like a cone in this moving picture and the original integral region cuts this cone completely. This means that the saddle point method is applicable.

Here is another example for the figure eight knot which is $(2, 2)$ double twist knot in Figure 11. This case is the most extremal one. For the other cases, the saddle points are closer to (π, π), and the contours deforms continuously with respect to (s, t).

Remark. The saddle point equation (11) always has a solution $x = y = \pi$, and the value $\mathrm{Im}\Big(2\pi(x + y) + 6(x - \pi)^2 - 2(y - \pi)^2 + \Phi(x, y)\Big)$ is equal to $\mathrm{Im}\,\Phi(\pi, \pi) = 7.3277$. This large value does not contribute to the sum (9) because we apply integral by part and therm for $m_1 = m_2 = 0$. Such phenomenon also happens for the Chen-Yang conjecture for the Turaev-Viro invariant. Any solution of the saddle point equation corresponds to a $\mathrm{SL}(2, \mathbb{C})$ representation, and the largest contributing terms comes from $|m_1| = |m_2| = 1$ term correspond to the geometric representation. The reason is that $2\pi m_i$ is the total angle around the i-th edge comes from the hyperbolic structure of the representation. The vanishing of the term for $m_i = 0$ is called the *big cancellation*, and here we give one explanation why such cancellation happens.

6 Neumann-Zagier function

The last thing we have to do is to show that the imaginary part of the value (12) is equal to the volume of the knot complement. To do this, we have to connect the results in

Contours of $\mathrm{Im}(2\pi(x+y)+6(x-\pi)^2-2(y-\pi)^2+\Phi(x,y))$.

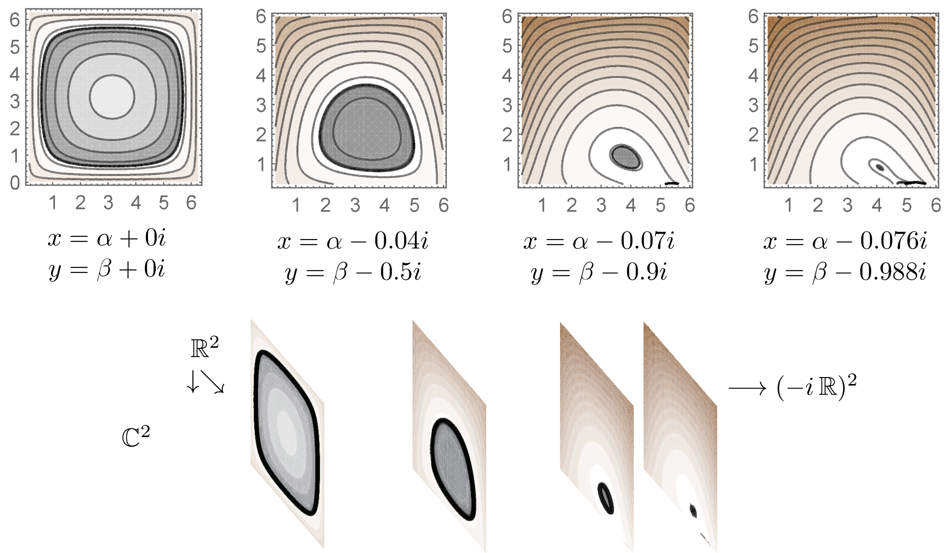

Figure 10: Check the condition for applying the saddle point method for $(6,2)$ double twist knot.

Sections 3 and Section 5, which is given by the following observation showing that the function Φ is equal to the Neumann-Zagier function in [8]. Therefore, the imaginary part of the value (12) is equal to the volume of the knot complement.

Observation 2. To get the saddle point equation (11), we have to compute $\frac{\partial \Phi}{\partial x}(x,y)$ and $\frac{\partial \Phi}{\partial y}(x,y)$. An actual computation shows that

$$\exp\Big(\frac{1}{i}\frac{\partial \Phi}{\partial x}(x,y)\Big)=p_2, \qquad \exp\Big(\frac{1}{i}\frac{\partial \Phi}{\partial y}(x,y)\Big)=q_4.$$

On the other hand, from the construction of the complexified tetrahedron, we see that p_2, q_4 are eigenvalues of $\rho(h_1)$ and $\rho'(h_2)$ where h_1, h_2 are elements of $\pi_1(S^3\setminus K)$ for meridians of the surgery components as in Figure 12 if we assign e^{ix}, e^{iy} to be the eigenvalues of the $\rho(g23)$ and $\rho'(g_{12})$ which represent the longitudes of the urgery components. Therefore, $\Phi(x,y)$ satisfies the same differential equation as the Neumann-Zagier function associated with the surgeries of two components of the Borromean rings, and the function $\Phi(x,y)$ must coincide with it up to a scalar. They are equal for $x=y=\pi$, which corresponds to the Borromean rings. So $\Phi(x,y)$ is equal to the Neumann-Zagier function.

7 Problems

Here is a list of problems for future work.

1. Generalize Theorem 1 to the complex volume $\mathrm{Vol}(S^3\setminus K)+\mathrm{CS}(S^3\setminus K)\sqrt{-1}$.
2. Generalize Theorem 1 to two-bridge knots.

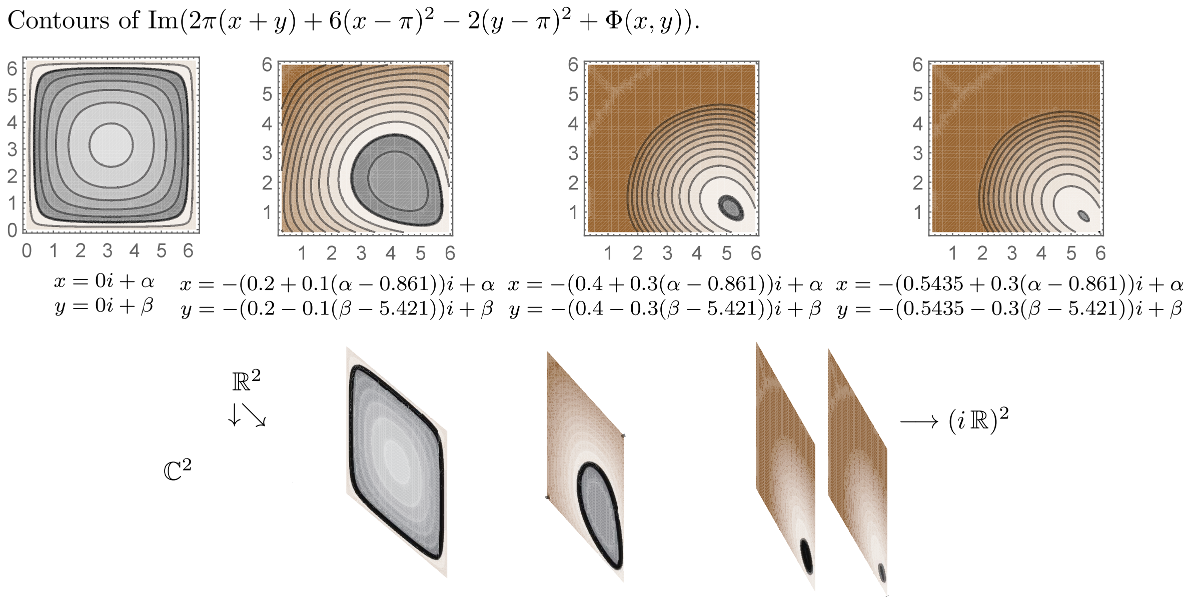

Figure 11: Check the condition for applying the saddle point method for the figure eight knot.

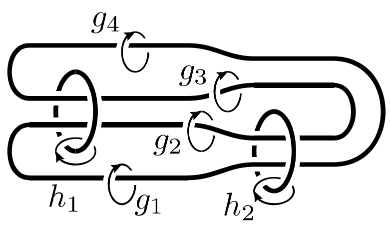

Figure 12: Elements of $\pi_1(S^3 \setminus B)$.

3. Generalize Theorem 1 to fully augmented links.
4. Prove the volume conjecture for general knot by using the face model for the colored Jones polynomial given in [5] and/or the ADO invariant given in [3].

Problem 1 may be solved by looking at the argument carefully. Problem 2 may be solved by the almost same argument here since the complement of the two-bridge knot can be decomposed into a combination of compleified teterahedrons whose shapes are similar to those for double twist knot. Two opposite edges have complexified parameters and other four edges are ideal points.

To solve problems 3 and 4, we may need more careful argument to check the condition for applying the saddle point method since the complexified tetrahedrons for these cases has more than two edges having complexified parameters.

References

[1] Y. Akutsu, T. Deguchi, T. Ohtsuki, *Invariants of colored links.* J. Knot Theory Ramifications **1** (1992), no. 2, 161–184.

[2] Q. Chen, S. Zhu, *On the asymptotic expansions of various quantum invariants II: the colored Jones polynomial of twist knots at the root of unity* $e^{\frac{2\pi\sqrt{-1}}{N+\frac{1}{M}}}$ *and* $e^{\frac{2\pi\sqrt{-1}}{N}}$. arXiv:2307.13670.

[3] F. Costantino, M. Murakami, *On the* $\mathrm{SL}(2,\mathbb{C})$ *quantum* $6j$*-symbols and their relation to the hyperbolic volume.* Quantum Topol. **4** (2013), no. 3, 303–351.

[4] R. M. Kashaev, *The hyperbolic volume of knots from the quantum dilogarithm.* Lett. Math. Phys. 39 (1997), no. 3, 269–275.

[5] A.N. Kirillov, N.Yu. Reshetikhin, *Representations of the algebra* $U_q(sl(2))$*, q-orthogonal polynomials and invariants of links.* Infinite-dimensional Lie algebras and groups (Luminy-Marseille, 1988), 285–339, Adv. Ser. Math. Phys., **7**, World Sci. Publ., Teaneck, NJ, 1989.

[6] H. Murakami, J. Murakami, *The colored Jones polynomials and the simplicial volume of a knot.* Acta Math. **186** (2001), 85–104.

[7] H. Murakami, J. Murakami, M. Okamoto, T. Takata, Y. Yokota, *Kashaev's conjecture and the Chern-Simons invariants of knots and links.* Experiment. Math. **11** (2002), 427–435.

[8] W. D. Neumann, D. Zagier, *Volumes of hyperbolic 3-manifolds.* Topology **24** (1985), 307–332.

[9] T. Ohtsuki, *On the asymptotic expansion of the Kashaev invariant of the* 5_2 *knot.* Quantum Topol. **7** (2016), 669–735,

[10] T. Ohtsuki, *On the asymptotic expansions of the Kashaev invariant of hyperbolic knots with seven crossings.* Internat. J. Math. 28 (2017), no. 13, 1750096, 143 pp.

[11] T. Ohtsuki, Y. Yokota, *On the asymptotic expansions of the Kashaev invariant of the knots with 6 crossings.* Mathematical Proceedings of the Cambridge Philosophical Society **165** (2018), 287–339.

Department of Mathematics
Faculty of Fundamental Science and Engineering
Waseda University
Tokyo 169-8555
JAPAN
E-mail address: `murakami@waseda.jp`

早稲田大学・基幹理工学部　村上 順